Published OnlineFirst February 4, 2016; DOI: 10.1158/1535-7163.MCT-15-0901

Large Molecule Therapeutics

Molecular Cancer Therapeutics

ABT-414, an Antibody–Drug Conjugate Targeting a Tumor-Selective EGFR Epitope

Andrew C. Phillips[1], Erwin R. Boghaert[1], Kedar S. Vaidya[1], Michael J. Mitten[1], Suzanne Norvell[2], Hugh D. Falls[1], Peter J. DeVries[1], Dong Cheng[1], Jonathan A. Meulbroek[1], Fritz G. Buchanan[1], Laura M. McKay[1], Neal C. Goodwin[3], and Edward B. Reilly[1]

Abstract

Targeting tumor-overexpressed EGFR with an antibody–drug conjugate (ADC) is an attractive therapeutic strategy; however, normal tissue expression represents a significant toxicity risk. The anti-EGFR antibody ABT-806 targets a unique tumor-specific epitope and exhibits minimal reactivity to EGFR in normal tissue, suggesting its suitability for the development of an ADC. We describe the binding properties and preclinical activity of ABT-414, an ABT-806 monomethyl auristatin F conjugate. *In vitro*, ABT-414 selectively kills tumor cells overexpressing wild-type or mutant forms of EGFR. ABT-414 inhibits the growth of xenograft tumors with high EGFR expression and causes complete regressions and cures in the most sensitive models. Tumor growth inhibition is also observed in tumor models with EGFR mutations, including activating mutations and those with the exon 2–7 deletion [EGFR variant III (EGFRvIII)], commonly found in glioblastoma multiforme. ABT-414 exhibits potent cytotoxicity against glioblastoma multiforme patient-derived xenograft models expressing either wild-type EGFR or EGFRvIII, with sustained regressions and cures observed at clinically relevant doses. ABT-414 also combines with standard-of-care treatment of radiation and temozolomide, providing significant therapeutic benefit in a glioblastoma multiforme xenograft model. On the basis of these results, ABT-414 has advanced to phase I/II clinical trials, and objective responses have been observed in patients with both amplified wild-type and EGFRvIII-expressing tumors. *Mol Cancer Ther; 15(4); 661–9. ©2016 AACR.*

Introduction

EGFR plays a causal role in the development and maintenance of many human carcinomas, with mutation and overexpression observed in a number of tumor types (1). Targeting EGFR is a clinically validated therapeutic strategy, with both mAbs and small molecules, having gained widespread use in lung, head and neck, colon, and pancreatic cancers (2). These EGFR-directed therapies have improved both progression-free and overall survival in a number of indications, including lung and colorectal cancer (3, 4). Despite the success of these inhibitors, significant numbers of patients with EGFR-positive tumors fail to respond to current EGFR-targeting therapeutics as a range of mutations (e.g., EGFR, KRas, BRaf, PI3K, and PTEN) may contribute to intrinsic or acquired resistance (5).

Antibody–drug conjugates (ADC) are a rapidly growing class of cancer drugs that combine the targeting properties of mAbs with the antitumor effects of potent cytotoxic drugs (6). Currently, microtubule inhibitors are clinically validated ADC payloads. Both Kadcyla (trastuzumab emtansine; Genentech) and Adcetris (brentuximab vedotin; Seattle Genetics) are FDA-approved ADC therapeutics, and more than 40 other ADCs have advanced to the clinic (7, 8). A microtubule inhibitor–based ADC targeting EGFR is an attractive therapeutic strategy that may improve on the activity of approved EGFR antagonists by circumventing resistance mediated by downstream signaling mutations. Nonetheless, marketed EGFR antibodies have limited potential for development as ADCs because their significant binding to normal tissue causes on-target toxicity (9). The most common toxicity of these agents is a characteristic skin rash, similar in appearance to acne, usually limited to the face, upper chest, and back. Other toxicities include diarrhea, constipation, stomatitis, fatigue, and electrolyte disturbances.

In contrast, ABT-806 is an EGFR-targeting antibody that binds a tumor-selective epitope of EGFR. ABT-806 is a humanized form of the monoclonal antibody mAb 806, which binds a cryptic epitope in the CR1 domain of EGFR that is accessible in tumors expressing amplified and overexpressed wild-type EGFR or the deletion mutant EGFR variant III (EGFRvIII; refs.10, 11). The low normal tissue binding of ABT-806 has been demonstrated in a phase I trial, where ABT-806 was well tolerated at the highest dose tested (24 mg/kg) with the absence of the characteristic EGFR inhibitor dermatologic adverse events (12). Further evidence of low normal tissue uptake of ABT-806 in patients is provided by its long half-life and dose-proportional pharmacokinetics. Other EGFR-targeting antibodies, including cetuximab and panitumumab, do not display dose-proportional pharmacokinetics and are characterized by significant target-mediated clearance (13–16). ABT-806, therefore, represents an attractive candidate for use as an ADC to deliver a potent cytotoxic payload to tumor cells expressing wild-type or mutant EGFR with limited toxicity to normal tissues.

[1]AbbVie, Oncology Discovery, North Chicago, Illinois. [2]TKIS, LLC., Long Grove, Illinois. [3]The Jackson Laboratory, Sacramento, California.

Note: Supplementary data for this article are available at Molecular Cancer Therapeutics Online (http://mct.aacrjournals.org/).

Corresponding Author: Edward B. Reilly, AbbVie, 1 N Waukegan Road, R460, North Chicago, IL 60064. Phone: 847-937-0815; Fax: 847-938-1336; E-mail: ed.reilly@abbvie.com

doi: 10.1158/1535-7163.MCT-15-0901

Published OnlineFirst February 4, 2016; DOI: 10.1158/1535-7163.MCT-15-0901

To assess the potential of ABT-806 as an antibody suitable for the development of an ADC, it was conjugated to the potent microtubule inhibitor, monomethyl auristatin F (MMAF), to generate ABT-414 (17). We describe here the preclinical characterization of ABT-414, including the assessment of activity in cell line–derived and patient-derived xenograft (PDX) models expressing either wild-type EGFR or EGFRvIII. The ability to target wild-type EGFR- and EGFRvIII-expressing tumors makes ABT-414 an attractive therapeutic candidate to treat solid tumors, including glioblastoma multiforme, where novel treatments are urgently needed (18, 19). The results presented here support further clinical development of ABT-414, which is currently in ongoing phase I/II trials, where objective responses (OR) in glioblastoma multiforme patients have been observed (20).

Material and Methods

Antibodies and proteins

Recombinant forms of EGFR (sEGFR wild-type ECD; sEGFRde2-7 ECD; $sEGFR^{C271A,C283A}$ ECD) were generated by AbbVie as described previously (11). Rituximab (Roche), cetuximab (Bristol-Myers Squibb), and temozolomide (Merck & Co., Inc.) were purchased. ABT-806 was produced by transient transfection of HEK-293-6E cells as described previously (11). Maleimidocaproyl MMAF (mcMMAF) was provided by Seattle Genetics, and conjugations to generate ABT-414 and control ADCs were performed by Seattle Genetics as described previously (21).

Cell culture

The tumor cell lines A431, NR6 fibroblasts, U87MGde2-7, and U87MG were obtained from the Ludwig Institute for Cancer Research (Melbourne, Australia). NCI-H292, HCT-15, FaDu, MDA-MD-468, A549, NCI-1703, NCI-H1441, LoVo, and SW48 cell lines were obtained from the ATCC. HCC827.ER.LMC was obtained from ATCC and serially passaged by subcutaneous injection into mouse flank to improve growth characteristics in mice. A431, NR6 fibroblast, NCI-H292, HCT-15, FaDu, HCC827.ER.LMC, NCI-H1703, NCI-H441, and SW48 cells were cultured in RPMI1640 supplemented with 10% FBS. U87MG and U87MGde2-7 were maintained in DMEM with high glucose, supplemented with 10% FBS and 1 mmol/L sodium pyruvate. U87MGde2-7 cells were maintained under selection with 400 μg/mL geneticin. MDA-MD-468 cells were maintained in DMEM supplemented with 10% FBS. A549 and LoVo cells were maintained in F-12K Nutrient Mixture supplemented with 10% FBS. SCC-15 cells were maintained in DMEM/F12K medium supplemented with 10% FBS. All cell lines were expanded in culture upon receipt and cryopreserved to provide cells at similar stage passages for all subsequent experiments. Cell lines were not authenticated in the 6 months before use; however, their EGFR expression levels were confirmed by FACS analysis.

Binding ELISA

Plates (96-well) were coated with 1 μg/mL of mouse 6x-His epitope tag mAb (4A12E4; Life Technologies) at 4°C overnight and then blocked using 10% SuperBlock (Pierce) in PBS with 0.05% Tween 20 (PBST) for 2 hours at room temperature. Plates were washed three times with PBST and incubated with 100 μL of soluble EGFR (sEGFR) extracellular domain (ECD) at 2 μg/mL for 1 hour at room temperature. Plates were washed three times with PBST, incubated with ABT-806 or ABT-414 as appropriate at room temperature for 1 hour, washed three times with PBST, and incubated with 100 μL of goat anti-human IgG-horseradish peroxidase (HRP; Pierce) at room temperature for 1 hour. After washing plates three times in PBST, 100 μL of 3,3′,5,5′-tetramethylbenzidine (TMB; Pierce) was added to each well and incubated at room temperature until color developed (~20 minutes). Reactions were stopped by the addition of 100 μL 1 N phosphoric acid, and optical density (OD) was read at 450 nm.

Phospho-EGFR ELISA

Cells were plated at 2×10^4 per well in collagen-coated 96-well plates in growth media. After 24 hours, cells were washed with serum-free media and serum starved for 4 hours. Where appropriate, cells were pretreated with mAb or ADC for 1 hour and then stimulated with Recombinant Human EGF (R&D Systems) for 10 minutes at 37°C. Following EGF stimulation, cells were washed twice with ice-cold PBS and lysed with 100 μL per well of cell lysis buffer (Cell Signaling Technology) supplemented with complete Protease Inhibitor Cocktail (Roche Diagnostics) and 0.1% NP40, and flash frozen at −80°C for at least 20 minutes. Phospho-EGFR levels were determined using a DuoSet IC ELISA (DYC1095; R&D Systems). Briefly, capture plates were generated by coating wells with 50 μL of an anti-EGFR antibody at 0.8 μg/mL, followed by blocking with PBS/1% BSA for 1 hour and washing three times with PBST. Cell lysates were added to capture plates and incubated at 4°C overnight. Plates were washed five times with PBST and incubated with pTyr-HRP for 1 hour. Plates were washed five times in PBST, and 100 μL of TMB peroxidase (HRP) substrate was added to each well and incubated at room temperature until color developed. Reactions were stopped by the addition of 100 μL 1 N HCl, and OD was read at 450 nm.

FACS analysis

Cells were harvested from flasks when approximately 80% confluent using Cell Dissociation Buffer (Life Technologies), washed once in PBS/1% FBS (FACS buffer), and then resuspended at 2.5×10^6 cells/mL in FACS buffer. Cells (100 μL) per well were added to a round-bottom 96-well plate. Ten microliters of a 10× concentration of mAb or ADC (final concentrations are indicated in the figures) was added, and the plate was incubated at 4°C for 1 hour. For competition, FACS FITC-conjugated ABT-806 was added to a final concentration of 100 nmol/L, and then wells were washed twice in FACS buffer, suspended in 100 μL of PBS/1% formaldehyde, and analyzed on a Becton Dickinson LSR II Flow Cytometer. For standard FACS, cells were washed twice with FACS buffer and resuspended in 50 μL of Alexa Fluor 488 Goat anti-Human IgG secondary antibody conjugate (11013; Life Technologies) diluted in FACS buffer. The plate was incubated at 4°C for 1 hour and washed twice with FACS buffer. Cells were resuspended in 100 μL of PBS/1% formaldehyde and analyzed on a LSR II Flow Cytometer. Data were analyzed using WinList flow cytometry analysis software.

Cytotoxicity assay

Cells were plated at 1×10^3 to 3×10^3 cells per well in complete growth medium containing 10% FBS in 96-well plates. The following day, medium was removed and replaced with fresh media containing titrations of antibodies or ADCs, and cells were incubated for 72 hours at 37°C in a humidified CO_2 incubator. Cell viability was then assessed using an ATPlite Luminescence

Published OnlineFirst February 4, 2016; DOI: 10.1158/1535-7163.MCT-15-0901

Assay (PerkinElmer) according to the manufacturer's instructions. A negative control ADC, rituximab-mcMMAF, was included in all assays to confirm that cell killing was antigen dependent. Rituximab was selected as a negative control as this antibody binds to CD20, an antigen that is not expressed in any of the solid tumor cell lines studied, does not recognize EGFR, and is not cross-reactive with mouse CD20.

Determination of receptor density

EGFR density was determined by means of Quantum Simply Cellular (QSC) microspheres (816; Bangs Laboratories). Briefly, cells grown to 80% to 90% confluence were harvested using Cell Dissociation Buffer (Life Technologies) or Versene (Life Technologies), transferred to 15 mL conical tubes, and combined with 6 mL FACS buffer [Ca^{2+}/Mg^{2+}-free Dulbecco's PBS (DPBS) + 1% FBS]. After centrifuging for 5 minutes at 300 × *g*, cells were resuspended in FACS buffer, counted, and then adjusted to a density of 2×10^6 cells/mL. 100 μL containing 2×10^5 cells were added to wells of a 96-well, round-bottom plate and incubated at 4°C with cetuximab (2 μg/mL) and rituximab (10 μg/mL) as positive and negative controls, respectively. Following 1-hour incubation with primary antibody, cells were centrifuged for 3 minutes at 300 × *g*, washed twice with FACS buffer, and then incubated 1 hour at 4°C with Alexa Fluor 488 Goat anti-Human IgG (11013; Life Technologies) diluted 1:100 in FACS buffer. Cells were then centrifuged for 3 minutes at 300 × *g*, washed twice with FACS buffer, and fixed with 100 μL per well of 1% formaldehyde in DPBS. The five standard bead populations from the QSC kit were prepared and stained with the 1:100 Alexa Fluor 488 Goat anti-Human IgG (11013; Life Technologies) according to the manufacturer's instructions. Bead standards resuspended in DPBS along with the fixed cell samples were then analyzed on a FACSCanto System (BD Biosciences). Data were interpreted via WinList software to generate geomean values. Geomean values for the bead populations were recorded in the provided lot-specific QuickCal template, and a regression associating fluorescence geomean value to bead antibody-binding capacity (ABC) value was calculated, resulting in a standard curve used to assign ABC (ABC or number of receptors) to stained cell samples.

In vivo studies

Female SCID, SCID-Beige, and nude mice were obtained from Charles River Laboratories. Ten mice were housed per cage. The body weight upon arrival was 20 to 22 g. Food and water were available *ad libitum*. Mice were acclimated to the animal facilities for a period of at least one week prior to commencement of experiments. Animals were tested in the light phase of a 12-hour light/dark schedule (lights on at 06:00 am). All experiments were conducted in compliance with AbbVie's Institutional Animal Care and Use Committee and the NIH Guide for Care and Use of Laboratory Animals Guidelines in a facility accredited by the Association for the Assessment and Accreditation of Laboratory Animal Care.

To generate xenografts, a suspension of viable tumors cells mixed with an equal amount of Matrigel (BD Biosciences) was injected subcutaneously into the flank of 6- to 8-week-old mice. The injection volume was 0.2 mL composed of a 1:1 mixture of S-MEM and Matrigel (BD Biosciences). Tumors were size matched at approximately 200 to 250 mm^3 unless otherwise indicated. Therapy began the day of or 24 hours after size matching the tumors. Mice weighed approximately 25 g at the onset of therapy. Each experimental group included 8 to 10 animals. Tumors were measured two to three times weekly. Measurements of the length (L) and width (W) of the tumor were obtained via electronic calipers, and the volume was calculated according to the following equation: $V = L \times W^2/2$. Mice were euthanized when tumor volume reached a maximum of 3,000 mm^3 or upon presentation of skin ulcerations or other morbidities, whichever occurred first. Host strains for each cell line and cell number in the inoculum are included in the Supplementary Table S1. For the SN0199 and SN0207 PDX models (The Jackson Laboratory), tumor fragments of 3 to 5 mm^3 at passage 3 (P3) were implanted subcutaneously in the right rear flank of NSG mice (The Jackson Laboratory) with a trocar (11). For all groups, tumor volumes were plotted only until the full set of animals remained on study. If animals had to be taken off study, the remaining animals were monitored for tumor growth until they reached defined endpoints.

Maximal tumor growth inhibition (TGI_{max}), expressed as a percentage, indicates the maximal divergence between the mean tumor volume of the test article–treated group and the control group treated with drug vehicle or isotype-matched nonbinding antibody. Tumor growth delay (TGD), expressed as a percentage, is the difference of the median time of the test article–treated group tumors to reach 1 cm^3 as compared with the control group.

Statistical analysis

IC_{50} and EC_{50} values were determined by nonlinear regression analysis of concentration response curves using GraphPad Prism 6.0. Data from experiments *in vivo* were analyzed using the two-way ANOVA with *post hoc* Bonferroni correction for TGI_{max} and the Mantel–Cox log-rank test for TGD (GraphPad Prism, GraphPad Software).

Results

ABT-414 retains binding and functional properties of ABT-806

ABT-414 was generated by the conjugation of MMAF to the interchain cysteines of ABT-806 via a noncleavable maleimidocaproyl linker with an average drug–antibody ratio of 3.8. To determine whether the unique tumor-selective binding properties of ABT-806 were retained following conjugation, a series of binding assays was performed to characterize ABT-414 binding. ABT-806 binding to various forms of recombinant and cell surface–expressed EGFR has been described previously, with high-affinity binding in an ELISA format observed to a mutant form of EGFR that exposes the epitope ($EGFR^{C271A,C283A}$; refs.11, 22). These binding characteristics are retained in ABT-414 with higher affinity binding to $EGFR^{C271A,C283A}$ (0.067 nmol/L for ABT-414 vs. 0.066 nmol/L for ABT-806) and lower affinity binding to wild-type EGFR (0.461 nmol/L for ABT-414 vs. 0.458 nmol/L for ABT-806). ABT-806 also has higher affinity for EGFRvIII, and this increased binding to EGFRvIII is also retained in ABT-414 (0.059 nmol/L vs. 0.060 nmol/L, respectively). FACS binding analyses of cells overexpressing wild-type EGFR, EGFRvIII, or $EGFR^{C271A,C283A}$ also confirmed the increased binding of ABT-414 for the mutant forms of the receptor, with binding characteristics essentially indistinguishable from ABT-806 (Fig. 1A and B). These results indicate that conjugation of ABT-806 to mcMMAF does not alter the binding properties of the parental antibody.

Published OnlineFirst February 4, 2016; DOI: 10.1158/1535-7163.MCT-15-0901

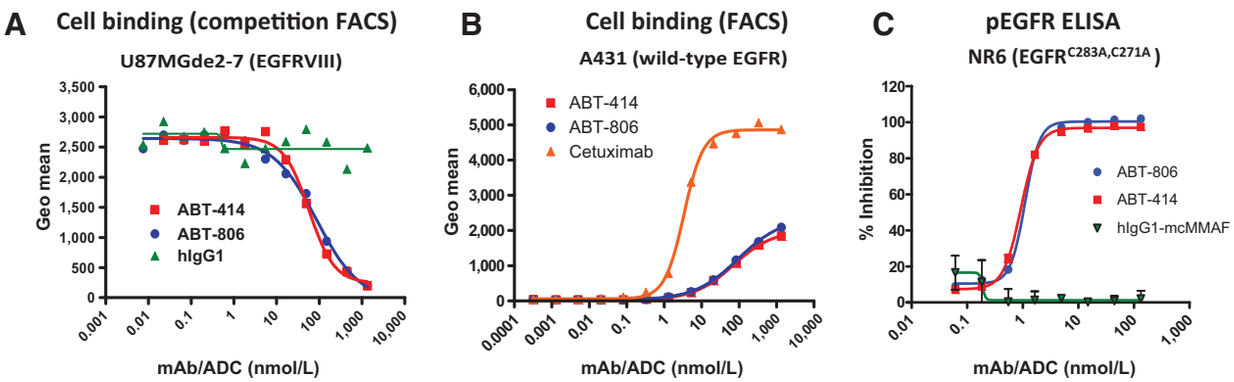

Figure 1.
ABT-414 retains ABT-806 binding and functional properties. A, the ability of ABT-414, ABT-806, and isotype control human IgG1 (hIgG1) to compete with labeled ABT-806 for binding to U87MGde2-7 cells was determined by FACS analysis. B, ABT-414, ABT-806, and cetuximab binding to A431 cells was assessed by FACS analysis. C, the effect of ABT-414 or ABT-806 treatment on EGF-mediated EGFR phosphorylation in a NR6 huEGFR^{C271A,C283A} cell line was assessed by phospho-EGFR (pEGFR) ELISA.

ABT-806 is an active therapeutic that inhibits EGFR signaling in both EGFR wild-type–overexpressed and EGFRvIII-expressing tumor cells (11). The impact of both ABT-806 and ABT-414 on EGFR signaling was compared to determine whether conjugation of the antibody to MMAF affected receptor signaling. As ABT-806 binds to wild-type EGFR poorly *in vitro*, a cell line expressing a mutant that exposes the epitope (EGFR^{C271A,C283A}) was used for these studies (11, 22). Both ABT-806 and ABT-414 bind these cells with high affinity and inhibit EGF-mediated signaling of this receptor with a similar potency (IC_{50} of 1.2 and 1.0 nmol/L, respectively; Fig. 1C).

ABT-414 *in vitro* cytotoxicity against EGFR-expressing cells

The cytotoxic activity of ABT-414 against a panel of human tumor cell lines expressing different forms and surface densities of EGFR was evaluated in cell killing assays. A FACS-based approach used to assess the levels of EGFR across these cell lines showed EGFR densities ranging from more than 1.6 million receptors per cell for the A431 cell line to 90,000 for the HCT-15 cell line (Fig. 2A). To confirm on-target killing by ABT-414, a nonbinding control human IgG1 conjugated to MMAF was used, and minimal cytotoxic activity was observed with this negative control in these assays (Fig. 2B).

ABT-414 displays significant cytotoxicity against tumor cells overexpressing wild-type or mutant forms of EGFR, with the growth of the most sensitive cell lines inhibited by single-digit nanomolar concentrations of ABT-414 (Table 1). Generally, there was good correlation between EGFR density and sensitivity to ABT-414–mediated killing, with those cells lines with more than 5×10^5 receptors per cell having IC_{50} values $\leq$21 nmol/L (Fig. 2C). ABT-414 also inhibits the growth of mouse fibroblasts engineered to overexpress human EGFR, whereas isogenic EGFR-null cells are resistant, further confirming the specificity of cell killing (Table 1). The cytotoxicity of ABT-414 *in vitro* results from delivery of the payload rather than from the efficacy of the antibody because unconjugated ABT-806 does not inhibit proliferation of tumor lines *in vitro* (Fig. 2B).

ABT-414 *in vivo* efficacy in wild-type and mutant EGFR–expressing models

In vivo efficacy of ABT-414 was characterized in multiple xenograft models derived from a variety of tumor types. ABT-414 treatment induced significant delay of tumor growth or tumor growth inhibition in 9 of 11 xenografts that were tested (Table 2). In all cases, the antitumor activity of ABT-414 was significantly

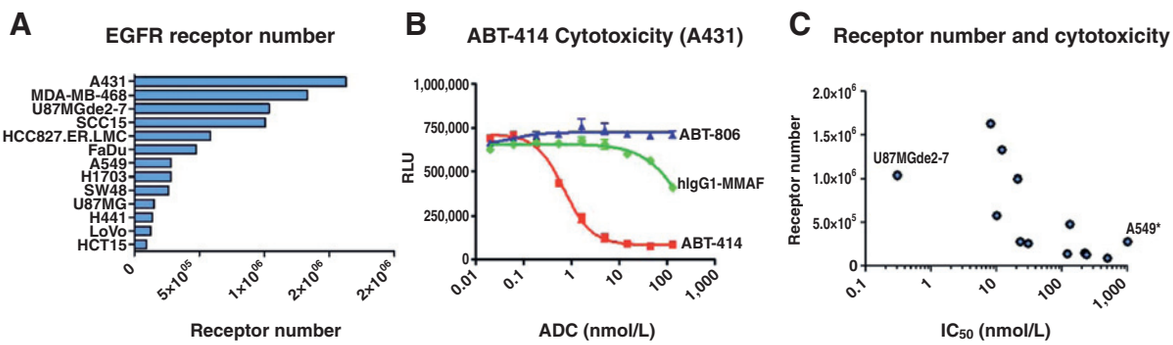

Figure 2.
ABT-414 cytotoxicity against EGFR-expressing tumor cell lines. A, EGFR number per cell (or ABC using cetuximab) was quantified for the cell lines indicated. B, cytotoxicity of ABT-414, ABT-806, and an isotype-matched negative control MMAF conjugate against the A431 cell line was assessed following incubation with drug for 72 hours. C, the correlation between EGFR receptor number and ABT-414 cytotoxicity is illustrated by plotting receptor number against IC_{50} for each cell line (*, A549 IC_{50} > 1,000 nmol/L, although plotted at 1,000 nmol/L).

Published OnlineFirst February 4, 2016; DOI: 10.1158/1535-7163.MCT-15-0901

Table 1. ABT-414 cytotoxicity in human tumor cell lines

Tumor cell line	Tumor type	EGFR Genotype	Cytotoxicity (nmol/L)[a]
A431	Vulvar epidermoid carcinoma	Wild-type amplified	8
MDA-MB-468	TN breast cancer	Wild-type amplified	12
U87MGde2-7	Glioblastoma multiforme	EGFRde2-7 (ectopic amplified)	0.3
SCC-15	HNSCC	Wild-type amplified	21
HCC827.ER.LMC	Lung adenocarcinoma	Wild-type, E746_A750 amplified	10
FaDu	Squamous cell carcinoma of the hypopharynx	Wild-type	130
A549	Lung carcinoma	Wild-type	>1,000
NCI-H1703	Lung squamous cell carcinoma	Wild-type	23
SW48	Colorectal adenocarcinoma	Wild-type	30
U87MG	Glioblastoma multiforme	Wild-type	222
NCI-H441	Lung adenocarcinoma	Wild-type	121
LoVo	Colorectal adenocarcinoma	Wild-type	234
HCT15	Colorectal adenocarcinoma	Wild-type	494
NR6	Mouse fibroblasts	EGFR-null	>1,000
NR6 EGFR wild-type	Mouse fibroblasts	EGFR wild-type	4

Abbreviations: TN, triple-negative; HNSCC; squamous cell carcinoma of the head and neck.
[a]Cell viability was determined following incubation with ABT-414 for 72 hours. The values represent IC_{50}s. Parental ABT-806 does not inhibit growth of any of these cell lines.

greater than that of parental ABT-806. Several tumor models were very sensitive to ABT-414 treatment, with regressions observed. In particular, ABT-414 mediated regressions and cures in the A431 xenograft squamous tumor model with amplified wild-type EGFR (Fig. 3A). We have previously shown that even repeated dosing with the parental ABT-806 mAb at 40 mg/kg does not induce regressions in this model, indicating that conjugation of MMAF significantly increases the potency (11). In addition, combining ABT-806 with the cell permeable monomethyl auristatin E (MMAE) toxin had minimal antitumor activity compared with either ABT-414 or ABT-806-MMAE (Supplementary Fig. S1B) indicating that conjugation is required for maximal efficacy.

ABT-414 was also highly effective against NCI-H1703 (squamous cell carcinoma of the lung), HCC827.ER.LMC (lung adenocarcinoma with EGFR-activating mutation), and SCC-15 (head and neck squamous cell carcinoma) xenografts (Table 2; Fig. 3B–D). In each of these models, sustained tumor regressions were observed after administration of $\leq$4 mg/kg ABT-414 when dosed every 4 days for a total of six doses (Q4D $\times$ 6 regimen). A distinct dosing regimen (1 mg/kg, Q4D $\times$ 3) was used to assess activity in the SCC-15 model, as higher doses of the unconjugated antibody can induce tumor regressions in this model (11). ABT-414 had a significantly greater response at 1 mg/kg than was observed with ABT-806 (Fig. 3D). A431, HCC827.ER.LMC, and SCC-15 cells harbor EGFR gene amplification, whereas NCI-H1703 overexpresses wild-type EGFR, indicating that ABT-414 can be effective against tumors with either overexpressed or amplified wild-type EGFR (23–26). In addition, HCC827 cells express the EGFR deE746-A750 deletion mutant, resulting in constitutive activation of the receptor (25). Not all EGFR-expressing xenografts were susceptible to inhibition by ABT-414 administration. HCT-15 and A549 xenografts, with lower levels of EGFR, did not respond to ABT-414 therapy (Table 2; Fig. 2).

Table 2. ABT-414 growth inhibition of xenograft tumors[a]

Xenograft	Dose (mg/kg)	TGI_{max} (%)	TGD (%)
A431	10	98	>792
FaDu	10	79	241
HCC827.ER.LMC	10	99	>694
SCC-15	1	79	133
LoVo	10	95	196
NCI-H1703	10	99	>546
NCI-H441	10	91	213
SW48	10	97	494
U87MGde2-7	10	99	>792
A549	10	19	0
HCT-15	10	24	23

[a]A comprehensive summary including results from different dosing regimens is available in the Supplementary Table S2.

In some models, the IgG-mcMMAF also resulted in a statistically significant TGD, although this was observed only at higher doses, and the responses were less durable than those observed with ABT-414 treatment. This growth inhibition by IgG-mcMMAF is likely a result of the enhanced permeability and retention effect resulting from antibody or ADC accumulation in tumors rather than the recognition of a tumor-associated antigen (27–29).

ABT-414 efficacy in glioblastoma multiforme models

As the prevalence of EGFRvIII and amplification of wild-type EGFR suggested glioblastoma as a potential target indication for ABT-806 and ABT-806–derived ADCs, the activity of ABT-414 was evaluated in the U87MGde2-7 glioblastoma multiforme model that expresses amplified exogenous EGFRvIII. ABT-414 elicited complete regressions and cures at 4 mg/kg dosing (Fig. 4A). In comparison, ABT-806 inhibited tumor growth but did not cause tumor regressions even when dosed at 20 mg/kg (Supplementary Fig. S1A)

ABT-414 activity was also evaluated in the glioblastoma multiforme PDX models SN0199 that coexpresses amplified EGFR wild-type and EGFRvIII and SN0207 that expresses wild-type EGFR. ABT-806 was not efficacious in the SN0207 model (Fig. 4B) and minimally affected SNO199 growth delay when dosed at 10 mg/kg, although it was more potent at higher doses (Fig. 4C; ref.11). In both SNO199 and SNO207 models, ABT-414 treatment caused significant tumor growth inhibition (SN0207, 87% TGI_{max}; SN0199, 96% TGI_{max}) and regression (Fig. 4B and C).

The ability of ABT-414 to combine with glioblastoma multiforme standard-of-care chemotherapy and radiotherapy was also evaluated in the U87MGde2-7 xenograft model. Suboptimal doses of ABT-414, temozolomide, and radiation were used in these studies to permit assessment of the triple combination. Addition of ABT-414 (1 mg/kg) to the clinical combination of temozolomide (1.5 mg/kg) and fractionated radiation (2 Gy)

Published OnlineFirst February 4, 2016; DOI: 10.1158/1535-7163.MCT-15-0901

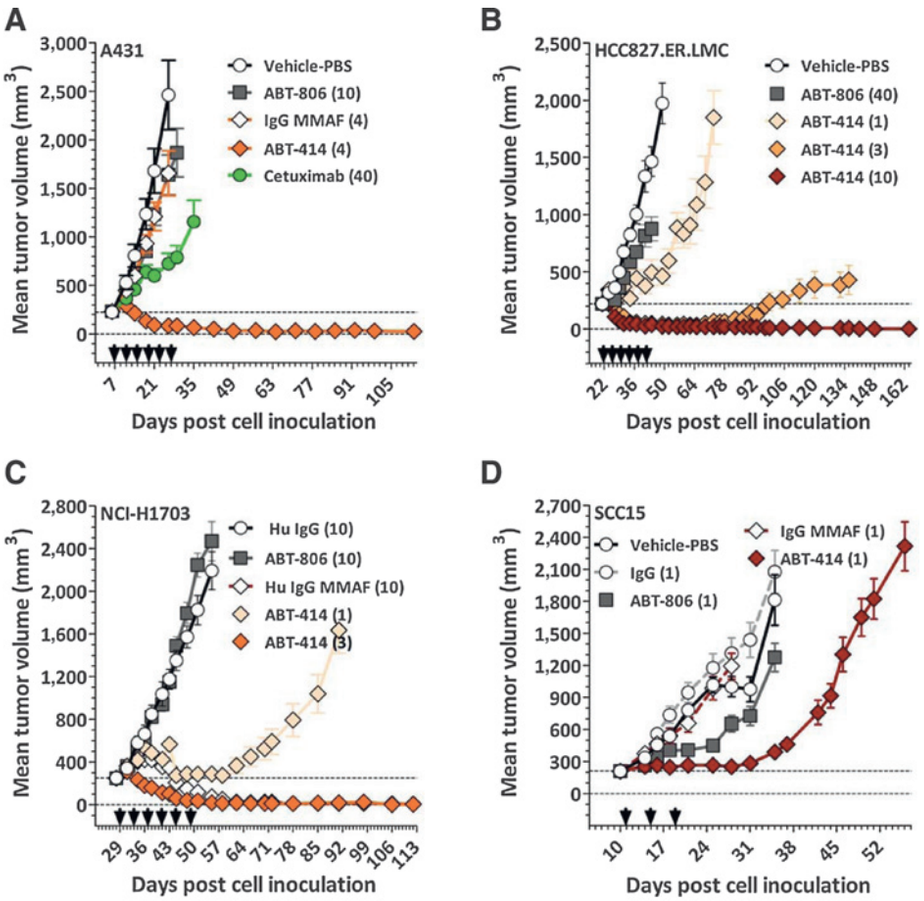

Figure 3.
ABT-414 efficacy against human tumor xenograft models. The *in vivo* potency of ABT-414 was evaluated in mice transplanted with A431 (A), HCC827.ER.LMC (B), NCI-H1703 (C), and SCC-15 (D) tumor cells. The ADCs or antibodies were administered at doses indicated in the figure on a Q4D × 6 schedule (A, B, and C) or a Q4D × 3 (D). Numbers in parentheses represent dose administered in mg/kg, and arrows indicate days of administration. Hu IgG, human IgG.

resulted in significant increase in tumor growth inhibition and tumor growth delay (Fig. 4C and D). The triple combination displayed significant benefit over the current standard of care, supporting the potential of enhanced efficacy of this combination regimen.

Discussion

The tumor specificity of ABT-806 makes it an attractive antibody for the development of an ADC. An auristatin payload was selected to conjugate to ABT-806 as this is the most widely used class of cytotoxins in clinical development (6). As glioblastoma multiforme was the most likely initial indication for successful clinical development, the cytotoxin MMAF was selected for clinical development because its low cell permeability relative to MMAE may minimize accumulation of free toxin in surrounding normal brain tissue and reduce the potential for neurotoxicity. In addition, although both MMAE and MMAF conjugates of ABT-806 demonstrated similar antitumor activity in multiple human tumor xenograft models, ABT-414 with the MMAF cytotoxin had slightly improved potency in a glioblastoma model (Supplementary Fig. S1A).

On the basis of the properties of the parental ABT-806, we anticipated that ABT-414 would be most effective in tumor cells with high levels of EGFR or those expressing EGFRvIII. This premise was supported by the results presented here, where all tumor models expressing more than 500,000 EGFR that were assessed *in vivo* showed potent responses to ABT-414. Models with fewer than 500,000 receptors showed variable responses. The differential response to ABT-414 may also reflect the sensitivity of different tumor types to the auristatin payload. For example, NCI-H1703 was highly responsive, whereas A549 with a similar receptor number was unresponsive. Of note, the most responsive xenografts to ABT-414 treatment also harbor amplified EGFR. In addition, the triple-negative breast cancer cell line MDA-MD-468 with amplified EGFR was highly sensitive to ABT-414 *in vitro* (30). These results suggest that amplification may be a useful selection tool to identify patients most likely to respond to ABT-414. A FISH-based assay to identify cancers harboring EGFR amplification has been implemented retrospectively as part of the ongoing ABT-414 phase I trials and is now being used prospectively in a phase II trial (20).

The efficacy of ABT-414 in models with amplified EGFR or EGFRvIII supports development of this model in glioblastoma multiforme, where approximately 50% of tumors have amplified EGFR and approximately 25% express EGFRvIII. Preclinical results show that ABT-414 is highly effective as monotherapy in the EGFRvIII-amplified U87MGde2-7 and the SNO199 PDX tumor models. ABT-414 is also very potent in the SN0207 glioblastoma multiforme PDX tumor model that expresses wild-type EGFR. Interestingly, the SN0207 model was unresponsive to both ABT-806 and cetuximab (11). ABT-414 also combines with

Published OnlineFirst February 4, 2016; DOI: 10.1158/1535-7163.MCT-15-0901

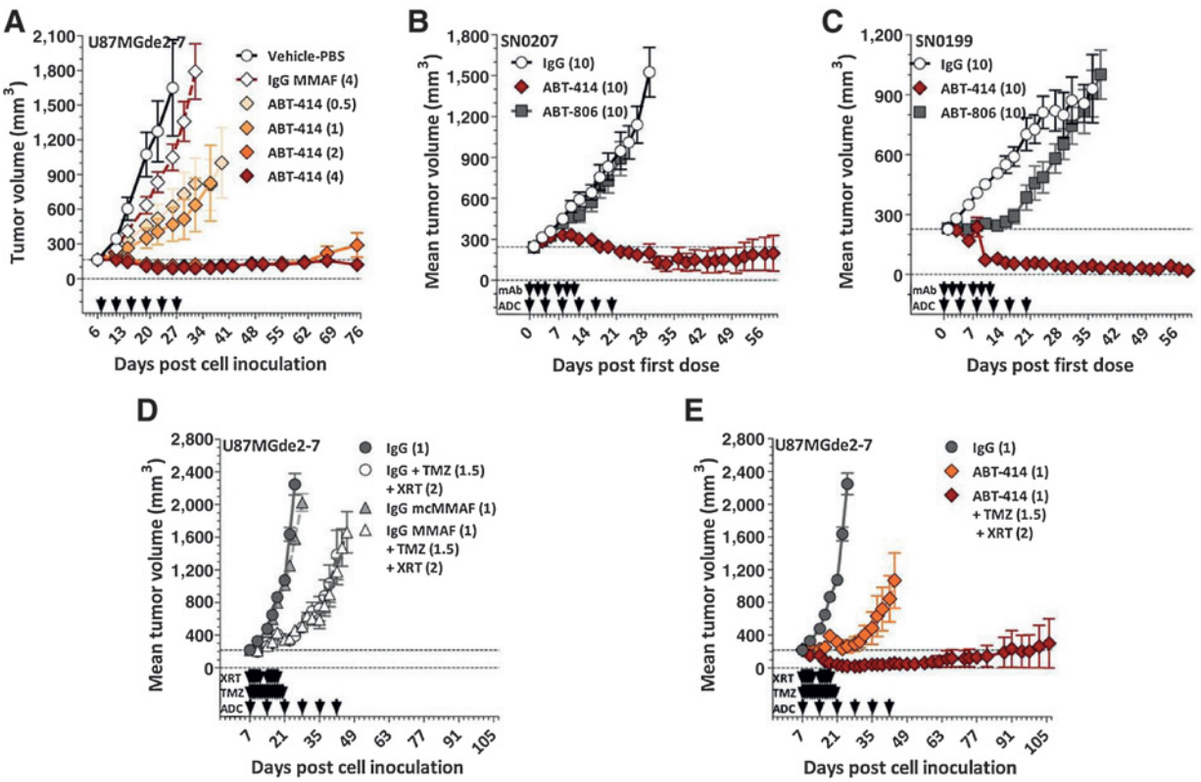

Figure 4.
ABT-414 efficacy against glioblastoma multiforme cell line and PDX models as monotherapy and in combination with temozolomide (TMZ) and fractionated radiation (XRT). The *in vivo* potency of ABT-414 was evaluated as monotherapy in mice transplanted with U87MGde2-7 (A), PDX SN0207 (B), and PDX SN0199 (C) and in combination with temozolomide and fractionated radiation in U87MGde2-7 (E). For the monotherapy arms, ABT-414 was dosed at the indicated doses at a Q4D × 6 regimen, whereas ABT-806 was dosed 10 mg/kg at a Monday–Wednesday–Friday × 2 regimen. For the combination arm, ABT-414 was dosed at 1.5 mg/kg Q4D × 6, temozolomide (1.5 mg/kg); QD × 14 and fractionated radiation (2 Gy); (QD × 5) × 2 with a two-day interval between cycles. The combination results from an isotype control MMAF (D) and ABT-414 (E) are plotted on separate graphs for clarity. Numbers in parentheses represent dose administered in mg/kg, and arrows indicate days of administration.

standard-of-care temozolomide/radiation in significantly delaying tumor growth of a glioblastoma xenograft model, providing additional support for development in glioblastoma multiforme.

ADC therapy of glioblastoma multiforme may potentially be limited by the blood brain barrier (BBB), which restricts transport of large molecules in the circulation to the brain. Previously, however, it was demonstrated that indium-labeled ABT-806 ([^{111}In]ABT-806), the radiolabeled parental antibody of ABT-414, showed specific tumor uptake in the brain in a glioma model grown orthotopically (11). In addition, phase I studies with both [^{111}In]chimeric 806 and [^{111}In]ABT-806 showed specific uptake in patients with brain tumors, demonstrating that this mAb crosses the BBB in these patients or that the BBB is sufficiently comprised or disrupted by the disease to enable uptake (31, 32). Collectively, these results provided a sound rationale for the investigation of ABT-414 in glioblastoma multiforme patient populations, and phase I and II trials are currently ongoing in this indication. ABT-414 has shown early clinical promise in recurrent glioblastoma multiforme with ORs, including complete responses observed, both as monotherapy and in combination with temozolomide in EGFR-amplified patients (20).

ABT-414 may also be efficacious in a subset of EGFR-expressing tumors other than glioblastoma multiforme. As ABT-414 efficacy in tumor models correlates with high EGFR expression levels, patients most likely to benefit from ABT-414 treatment are expected to be those with amplified or very highly overexpressed wild-type EGFR-tumors. EGFR amplification occurs in many tumor types, including lung and head and neck cancers, although with a typically lower copy number and at a frequency much less common than observed in glioblastoma multiforme (33, 34). Consistent with these observations, in the ABT-414 phase I studies outside of the glioblastoma multiforme setting, a single partial response was observed in a patient with triple-negative breast cancer, and the tumor was retrospectively determined to have wild-type amplified EGFR (35). EGFRvIII expression has also been reported in several tumor types in addition to glioblastoma multiforme, suggesting utility of ABT-414 in these settings, although our data are consistent with low prevalence outside of glioblastoma multiforme (36–40). In addition, lung cancer tumors harboring EGFR-activating mutations that render them sensitive to tyrosine kinase inhibitors may also be sensitive to ABT-414, as the site of the mutation in the kinase domain of EGFR is distinct from the ECD recognized by the antibody (11, 22). Preclinical results demonstrate that ABT-414 is active against the HCC827 lung tumor model harboring the EGFR-activating E746_A750 EGFR deletion mutation and a PDX model (LG0703)

Published OnlineFirst February 4, 2016; DOI: 10.1158/1535-7163.MCT-15-0901

expressing the L858R mutation (data not shown). The efficacy of ABT-414 against tumors with different forms of EGFR distinguishes it from EGFRvIII-specific ADCs, such as the recently described AMG 595 (41).

In summary, ABT-414 is a promising therapeutic with unique targeting capabilities. The preclinical data support the continued clinical evaluation of ABT-414 in EGFR-expressing malignancies. In this context, it will be interesting to monitor the ongoing frequency and durability of responses in ABT-414 clinical trials.

Disclosure of Potential Conflicts of Interest

N.C. Goodwin is the Vice President of Corporate Research and Development at Champions Oncology, Inc. No potential conflicts of interest were disclosed by the other authors.

Authors' Contributions

Conception and design: A.C. Phillips, E.R. Boghaert, K.S. Vaidya, S. Norvell, D. Cheng, J.A. Meulbroek, F.G. Buchanan, E.B. Reilly
Development of methodology: A.C. Phillips, K.S. Vaidya, S. Norvell, P.J. DeVries, D. Cheng, J.A. Meulbroek
Acquisition of data (provided animals, acquired and managed patients, provided facilities, etc.): A.C. Phillips, K.S. Vaidya, M.J. Mitten, S. Norvell, H.D. Falls, P.J. DeVries, D. Cheng, J.A. Meulbroek, L.M. McKay, N.C. Goodwin
Analysis and interpretation of data (e.g., statistical analysis, biostatistics, computational analysis): A.C. Phillips, E.R. Boghaert, K.S. Vaidya, S. Norvell, H.D. Falls, P.J. DeVries, D. Cheng, J.A. Meulbroek, N.C. Goodwin, E.B. Reilly
Writing, review, and/or revision of the manuscript: A.C. Phillips, E.R. Boghaert, K.S. Vaidya, M.J. Mitten, H.D. Falls, P.J. DeVries, D. Cheng, J.A. Meulbroek, F.G. Buchanan, L.M. McKay, N.C. Goodwin, E.B. Reilly
Administrative, technical, or material support (i.e., reporting or organizing data, constructing databases): H.D. Falls, D. Cheng, E.B. Reilly
Study supervision: A.C. Phillips, E.R. Boghaert, K.S. Vaidya, D. Cheng, F.G. Buchanan, N.C. Goodwin, E.B. Reilly

Acknowledgments

The authors thank Lenette Paige for her excellent technical assistance.

Grant Support

The design, study conduct, and financial support for the study were provided by AbbVie.

The costs of publication of this article were defrayed in part by the payment of page charges. This article must therefore be hereby marked *advertisement* in accordance with 18 U.S.C. Section 1734 solely to indicate this fact.

Received November 11, 2015; revised January 22, 2016; accepted January 26, 2016; published OnlineFirst February 4, 2016.

References

1. Burgess AW. EGFR family: structure physiology signalling and therapeutic targets. Growth Factors 2008;26:263–74.
2. Mendelsohn J, Baselga J. Epidermal growth factor receptor targeting in cancer. Semin Oncol 2006;33:369–85.
3. Enrique AA, Gema PC, Jeronimo JC, Auxiliadora GE. Role of anti-EGFR target therapy in colorectal carcinoma. Front Biosci 2012;4:12–22.
4. Landi L, Cappuzzo F. Pharmacotherapy targeting the EGFR oncogene in NSCLC. Expert Opin Pharmacother 2014;15:2293–305.
5. Chong CR, Janne PA. The quest to overcome resistance to EGFR-targeted therapies in cancer. Nat Med 2013;19:1389–400.
6. Leal M, Sapra P, Hurvitz SA, Senter P, Wahl A, Schutten M, et al. Antibody-drug conjugates: an emerging modality for the treatment of cancer. Ann N Y Acad Sci 2014;1321:41–54.
7. Okeley NM, Alley SC, Senter PD. Advancing antibody drug conjugation: from the laboratory to a clinically approved anticancer drug. Hematol Oncol Clin North Am 2014;28:13–25.
8. Baron JM, Boster BL, Barnett CM. Ado-trastuzumab emtansine (T-DM1): a novel antibody-drug conjugate for the treatment of HER2-positive metastatic breast cancer. J Oncol Pharm Pract 2015;21:132–42.
9. Li T, Perez-Soler R. Skin toxicities associated with epidermal growth factor receptor inhibitors. Target Oncol 2009;4:107–19.
10. Gan HK, Burgess AW, Clayton AH, Scott AM. Targeting of a conformationally exposed, tumor-specific epitope of EGFR as a strategy for cancer therapy. Cancer Res 2012;72:2924–30.
11. Reilly EB, Phillips AC, Buchanan FG, Kingsbury G, Zhang Y, Meulbroek JA, et al. Characterization of ABT-806, a humanized tumor-specific anti-EGFR monoclonal antibody. Mol Cancer Ther 2015;14:1141–51.
12. Cleary JM, Reardon DA, Azad N, Gandhi L, Shapiro GI, Chaves J, et al. A phase 1 study of ABT-806 in subjects with advanced solid tumors. Invest New Drugs 2015;33:671–8.
13. Sharma S, Mittapalli RK, Holen KD, Xiong H. Population pharmacokinetics of ABT-806, an investigational anti-epidermal growth factor receptor (EGFR) monoclonal antibody, in advanced solid tumor types likely to either over-express wild-type EGFR or express variant III mutant EGFR. Clin Pharmacokinet 2015;54:1071–81.
14. Baselga J, Pfister D, Cooper MR, Cohen R, Burtness B, Bos M, et al. Phase I studies of anti-epidermal growth factor receptor chimeric antibody C225 alone and in combination with cisplatin. J Clin Oncol 2000;18:904–14.
15. Shin DM, Donato NJ, Perez-Soler R, Shin HJ, Wu JY, Zhang P, et al. Epidermal growth factor receptor-targeted therapy with C225 and cisplatin in patients with head and neck cancer. Clin Cancer Res 2001;7:1204–13.
16. Yang BB, Lum P, Chen A, Arends R, Roskos L, Smith B, et al. Pharmacokinetic and pharmacodynamic perspectives on the clinical drug development of panitumumab. Clin Pharmacokinet 2010;49:729–40.
17. Doronina SO, Bovee TD, Meyer DW, Miyamoto JB, Anderson ME, Morris-Tilden CA, et al. Novel peptide linkers for highly potent antibody-auristatin conjugate. Bioconjug Chem 2008;19:1960–3.
18. Henson JW. Treatment of glioblastoma multiforme: a new standard. Archiv Neurol 2006;63:337–41.
19. Blumenthal DT, Schulman SF. Survival outcomes in glioblastoma multiforme, including the impact of adjuvant chemotherapy. Expert Rev Neurother 2005;5:683–90.
20. Gan HK, Fichtel L, Lassman AB, Merrell R, Van Den Bent MJ, Kumthekar P, et al. A phase 1 study evaluating ABT-414 in combination with temozolomide (TMZ) for subjects with recurrent or unresectable glioblastoma (GBM). J Clin Oncol 2014;35:2021.
21. Doronina SO, Mendelsohn BA, Bovee TD, Cerveny CG, Alley SC, Meyer DL, et al. Enhanced activity of monomethylauristatin F through monoclonal antibody delivery: effects of linker technology on efficacy and toxicity. Bioconjug Chem 2006;17:114–24.
22. Garrett TP, Burgess AW, Gan HK, Luwor RB, Cartwright G, Walker F, et al. Antibodies specifically targeting a locally misfolded region of tumor associated EGFR. Proc Natl Acad Sci U S A 2009;106:5082–7.
23. Merlino GT, Ishii S, Whang-Peng J, Knutsen T, Xu YH, Clark AJ, et al. Structure and localization of genes encoding aberrant and normal epidermal growth factor receptor RNAs from A431 human carcinoma cells. Mol Cell Biol 1985;5:1722–34.
24. Merlino GT, Xu YH, Richert N, Clark AJ, Ishii S, Banks-Schlegel S, et al. Elevated epidermal growth factor receptor gene copy number and expression in a squamous carcinoma cell line. J Clin Invest 1985;75:1077–9.
25. Amann J, Kalyankrishna S, Massion PP, Ohm JE, Girard L, Shigematsu H, et al. Aberrant epidermal growth factor receptor signaling and enhanced sensitivity to EGFR inhibitors in lung cancer. Cancer Res 2005;65:226–35.
26. Ramos AH, Dutt A, Mermel C, Perner S, Cho J, Lafargue CJ, et al. Amplification of chromosomal segment 4q12 in non-small cell lung cancer. Cancer Biol Ther 2009;8:2042–50.
27. Boghaert ER, Khandke K, Sridharan L, Armellino D, Dougher M, Dijoseph JF, et al. Tumoricidal effect of calicheamicin immuno-conjugates using a passive targeting strategy. Int J Oncol 2006;28:675–84.
28. Heneweer C, Holland JP, Divilov V, Carlin S, Lewis JS. Magnitude of enhanced permeability and retention effect in tumors with different phenotypes: 89Zr-albumin as a model system. J Nuclear Med 2011;52:625–33.

29. Fang J, Nakamura H, Maeda H. The EPR effect: Unique features of tumor blood vessels for drug delivery, factors involved, and limitations and augmentation of the effect. Adv Drug Deliv Rev 2011;63: 136–51.
30. Filmus J, Pollak MN, Cailleau R, Buick RN. MDA-468, a human breast cancer cell line with a high number of epidermal growth factor (EGF) receptors, has an amplified EGF receptor gene and is growth inhibited by EGF. Biochem Biophys Res Commun 1985;128:898–905.
31. Scott AM, Lee FT, Tebbutt N, Herbertson R, Gill SS, Liu Z, et al. A phase I clinical trial with monoclonal antibody ch806 targeting transitional state and mutant epidermal growth factor receptors. Proc Natl Acad Sci U S A 2007;104:4071–6.
32. Gan HK, Burge ME, Solomon BJ, Holen KH, Zhang Y, Ciprotti M, et al. A phase I and biodistribution study of ABT-806i, an 111indium-labeled conjugate of the tumor-specific anti-EGFR antibody ABT-806. J Clin Oncol 31, 2013 (suppl; abstr 2520).
33. The Cancer Genome Atlas Network. Comprehensive genomic characterization of head and neck squamous cell carcinomas. Nature 2015;517: 576–82.
34. The Cancer Genome Atlas Research Network. Comprehensive genomic characterization of squamous cell lung cancers. Nature 2012;489: 519–25.
35. Goss GD, Vokes EE, Gordon MS, Gandhi L, Papadopoulos KP, Rasco DW, et al. ABT-414 in patients with advanced solid tumors likely to overexpress the epidermal growth factor receptor (EGFR). J Clin Oncol 2015;33:2510.
36. Khattri A, Zuo Z, Bragelmann J, Keck MK, El Dinali M, Brown CD, et al. Rare occurrence of EGFRvIII deletion in head and neck squamous cell carcinoma. Oral Oncol 2015;51:53–8.
37. Sok JC, Coppelli FM, Thomas SM, Lango MN, Xi S, Hunt JL, et al. Mutant epidermal growth factor receptor (EGFRvIII) contributes to head and neck cancer growth and resistance to EGFR targeting. Clin Cancer Res 2006; 12:5064–73.
38. Sasaki H, Kawano O, Endo K, Yukiue H, Yano M, Fujii Y. EGFRvIII mutation in lung cancer correlates with increased EGFR copy number. Oncol Rep 2007;17:319–23.
39. Cunningham MP, Essapen S, Thomas H, Green M, Lovell DP, Topham C, et al. Coexpression, prognostic significance and predictive value of EGFR, EGFRvIII and phosphorylated EGFR in colorectal cancer. Int J Oncol 2005;27:317–25.
40. Wikstrand CJ, Hale LP, Batra SK, Hill ML, Humphrey PA, Kurpad SN, et al. Monoclonal antibodies against EGFRvIII are tumor specific and react with breast and lung carcinomas and malignant gliomas. Cancer Res 1995; 55:3140–8.
41. Hamblett KJ, Kozlosky CJ, Siu S, Chang WS, Liu H, Foltz IN, et al. AMG 595, an anti-EGFRvIII antibody-drug conjugate, induces potent antitumor activity against EGFRvIII-expressing glioblastoma. Mol Cancer Ther 2015; 14:1614–24.

Published OnlineFirst February 4, 2016; DOI: 10.1158/1535-7163.MCT-15-0901

Molecular Cancer Therapeutics

ABT-414, an Antibody–Drug Conjugate Targeting a Tumor-Selective EGFR Epitope

Andrew C. Phillips, Erwin R. Boghaert, Kedar S. Vaidya, et al.

Mol Cancer Ther 2016;15:661-669. Published OnlineFirst February 4, 2016.